Journal of Advanced Research (2016) 7, 597–610

Cairo University

Journal of Advanced Research

ORIGINAL ARTICLE

# Biosorptive uptake of $Fe^{2+}$, $Cu^{2+}$ and $As^{5+}$ by activated biochar derived from *Colocasia esculenta*: Isotherm, kinetics, thermodynamics, and cost estimation

**Soumya Banerjee [a], Shraboni Mukherjee [a], Augustine LaminKa-ot [b], S.R. Joshi [b], Tamal Mandal [a], Gopinath Halder [a,*]**

[a] *Department of Chemical Engg, National Institute of Technology Durgapur, West Bengal, India*
[b] *Department of Biotechnology and Bioinformatics, North-Eastern Hill University, Shillong, India*

## GRAPHICAL ABSTRACT

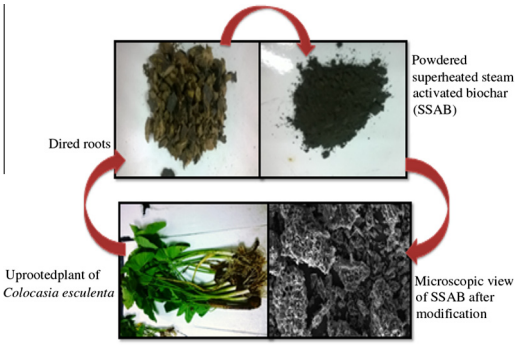


## ARTICLE INFO

*Article history:*
Received 24 April 2016
Received in revised form 12 June 2016

## ABSTRACT

The adsorptive capability of superheated steam activated biochar (SSAB) produced from *Colocasia esculenta* was investigated for removal of $Cu^{2+}$, $Fe^{2+}$ and $As^{5+}$ from simulated coal mine wastewater. SSAB was characterized by scanning electron microscopy, Fourier transform

* Corresponding author. Fax: +91 3432754078.
E-mail address: gopinath_haldar@yahoo.co.in (G. Halder).
Peer review under responsibility of Cairo University.

Production and hosting by Elsevier

http://dx.doi.org/10.1016/j.jare.2016.06.002

Accepted 13 June 2016
Available online 17 June 2016

*Keywords:*
Metal removal
Activated biochar
Adsorption
Desorption
Regeneration
Cost estimation

infrared spectroscopy and Brunauer–Emmett–Teller analyser. Adsorption isotherm indicated monolayer adsorption which fitted best in Langmuir isotherm model. Thermodynamic study suggested the removal process to be exothermic, feasible and spontaneous in nature. Adsorption of $Fe^{2+}$, $Cu^{2+}$ and $As^{5+}$ on to SSAB was found to be governed by pseudo-second order kinetic model. Efficacy of SSAB in terms of metal desorption, regeneration and reusability for multiple cycles was studied. Regeneration of metal desorbed SSAB with 1 N sodium hydroxide maintained its effectiveness towards multiple metal adsorption cycles. Cost estimation of SSAB production substantiated its cost effectiveness as compared to commercially available activated carbon. Hence, SSAB could be a promising adsorbent for metal ions removal from aqueous solution.



## Introduction

Increase in metal toxicity due to advancement in industrialization and excessive exploitation of natural resources has created a major environmental concern for the past couple of decades. Natural resources such as groundwater are being contaminated due to progressive urbanization which resulted in depletion of portable water in many parts of the world [1,2]. Among various industries such as tanning, electroplating, smelting, and wood polishing, mining has been considered as one of the major sources of metal discharge into natural water systems [3]. This has been one of the oldest anthropogenic activities where coal is used as a source of energy. Due to extensive open cast and underground mining, quality of groundwater has been affected severely. Generation of leachates and dumping of coal in mining areas have also contributed towards contamination of underground water table thereby deteriorating its quality [4]. Ores containing metals are transported from earth crust onto the mine surface and from there it reaches adjoining water bodies by both anthropogenic and physical activities [5]. Hence contamination of groundwater has become a serious environmental issue since it leads to an abrupt increase in heavy metal concentration within other natural resources [6]. In human body, some of these heavy metals are required in trace amounts as daily supplements which become toxic if the amount exceeds [7]. Severe rules have been imposed by various authorities on the discharge of heavy metals in open topography and water systems [8]. Among several metal discharges into water bodies, concentrations of iron ($Fe^{2+}$), copper ($Cu^{2+}$) and arsenic ($As^{5+}$) have been increasing rapidly in groundwater [9–11]. Different organizations viz. United State Environmental Protection Agency (USEPA), World Health Organization (WHO), Indian Standard Institutions (ISI), Indian Council of Medical Research (ICMR) and Central Pollution Control Board (CPCB) which deal with environmental pollution and resources, have prescribed the permissible limits and harmful effects of these three metal ions on human health [12–15] which are tabulated in Table 1.

Several methods have already been reported on removal of $Fe^{2+}$, $Cu^{2+}$ and $As^{5+}$ from aqueous solutions, viz., ion-exchange [16], membrane filtration [17], reverse osmosis [18], chemical precipitation [19], and adsorption [20]. Among these methods, adsorption is considered to be a potential technique in removal and recovery of metal ions from aqueous solution [21]. At lower metal concentration, some of these conventional technologies have been reported to be ineffective whereas metal removal by adsorption is possible even at a lower concentration of 1 mg/L [22,23]. Since adsorption is a metabolism free process, dried biomass of plants can be effectively used as adsorbents because they remain unaffected by the toxic effect of heavy metals [24].

Various adsorbents derived from microbes and plant biomasses such as *Saccharomyces cerevisiae*, *Ceratophyllum demersum*, *Myriophyllum spicatum*, *Potamogeton lucens*, *Salvinia herzogii*, and *Eichhornia crassipes* have been used in metal removal [25–28]. The cost of using microbe-based biomass is quite high compared to plant-based biomass. Therefore, more attention is being paid by researchers on plant biomass since it can be easily processed with least production cost [29]. Leaves of *Ficus religiosa*, coffee beans, coconut shell and coir, jute stick, cereals, lemon juice derived zinc oxide nanoparticles, etc., have been used to prepare activated carbon for the removal of $Fe^{2+}$, $Cu^{2+}$ and $As^{5+}$ from water [30–32]. However, the metal uptake capability of activated biochar developed from *Colocasia esculenta* has not been reported yet.

Therefore, the present study aimed towards preparation and characterization of superheated steam activated biochar of *C. esculenta* roots for its application in $Fe^{2+}$, $Cu^{2+}$ and $As^{5+}$ removal under the influence of six process parameters viz. pH, temperature, adsorbent dose, initial metal concentra-

**Table 1** Permissible limits and health risk of $Fe^{2+}$, $Cu^{2+}$ and $As^{5+}$.

| Metal ion | USEPA (mg/L) | WHO (mg/L) | ISI (mg/L) | ICMR (mg/L) | CPCB (mg/L) | Health risk |
|---|---|---|---|---|---|---|
| $Fe^{2+}$ | – | 0.1 | 0.3 | 1.0 | 1.0 | Haemorrhagic necrosis sloughing of mucosal area in stomach haemochromatosis |
| $Cu^{2+}$ | 1.3 | 1.0 | 0.05 | 1.5 | 1.5 | Gastrointestinal disorder, irritation of nose, mouth, eyes, headache |
| $As^{5+}$ | 0.05 | 1.5 | 1.5 | 0.05 | – | Abdominal pain, vomiting, diarrhea, muscular pain, flushing of skin, skin cancer |

tion, agitation speed and contact time in a series of batch adsorption studies. Desorption and regeneration of spent superheated steam activated biochar (SSAB) was also carried out to assess its reusability. In addition, the cost involved in SSAB preparation was calculated to account for its cost effectiveness.

## Material and method

### *Adsorbent preparation*

Removal of $Cu^{2+}$, $Fe^{2+}$ and $As^{5+}$ was studied using activated biochar prepared from the roots of *C. esculenta*. *C. esculenta* commonly known as "Taro" is a perennial plant which is widely available in various parts of Asia, Africa and in other tropical region. It is abundantly available in marshy areas, ditches, ponds and lakes [33]. Before adsorbent preparation, the roots were separated from the stem, diced into uniform shape, washed thoroughly under running tap water and dried for 2 days under sunlight during the daytime followed by drying in hot air oven (S.C. Dey Instruments Manufacturer, Kolkata, India) at night at 100 °C. The roots were initially sun dried before drying it in hot air oven to prevent it from decomposition which might affect its adsorption efficiency.

It is important to determine the carbon quantity of a sample before it is set for carbonization. Determination of carbon quantity gives a firsthand idea on the amount of carbon which can be obtained for adsorbent preparation. Total carbon content, total volatile matter content and ash content of the root sample were calculated by proximate analysis in accordance with standard ASTM method [34]. For carbonization, the dehydrated roots were placed inside a spherical shelled muffle furnace (Sonuu Instruments Mfg. Co., Kolkata, India) at 350 °C for about 45 min which continued further in the lag phase for 40 min at same temperature. After lag phase, the roots were further heated at elevated temperature with an increase in temperature at 10 °C per minute till it reached 600 °C. From 600 °C, carbonization of the roots was initiated which lasted for 45 min and further extended to a lag phase at same temperature for 20 min.

After carbonization the furnace temperature was increased up to 700 °C with a heating rate of 10 °C per minute for activation. In our study, physical activation was chosen over chemical activation because physical activation is more convenient in terms of cost and time since chemical activation by acids (HCl, $H_2SO_4$, etc.) requires more time in pre and post treatment of the samples [35]. Therefore, the biochar was steam activated by passing superheated steam under a controlled rate of 1.5 kg/cm$^2$ at 700 °C for 45 min. After 45 min of steam flow, the lag phase was maintained for 20 min at 700 °C. After completion of the activation process, the activated sample was ground using an electronic grinder into a particle size of 450 μm by screening it through standard sieves. SSAB was then kept inside an air tight container for further use.

### *Preparation of stock solution*

Stock solutions of the three metal ions viz., $Fe^{2+}$, $Cu^{2+}$ and $As^{5+}$ were prepared with analytical grade ferrous sulphate ($FeSO_4{\cdot}5H_2O$), copper sulphate ($CuSO_4{\cdot}7H_2O$) and sodium arsenate ($Na_2AsO_4$) purchased from Merck, Kolkata, India. 1000 mg/L stock solution of each metal ion was prepared with 2.7 g, 2.5 g and 4.16 g of $FeSO_4{\cdot}5H_2O$, $CuSO_4{\cdot}7H_2O$ and $Na_2AsO_4$ respectively in 1000 mL of deionized water (obtained from laboratory setup) in three separate volumetric flasks. The stock solutions were kept at acidic pH (below 6) to prevent it from metal precipitation. 1 N hydrochloric acid and 1 N sodium hydroxide obtained from Merck, Kolkata, India, were used to maintain the solution pH.

### *Determination of point of zero charge ($pH_{pzc}$)*

0.5 g of SSAB was added in 30 mL of deionized water and agitated and final pH of the slurry after 24 h was found to be 6.5. $pH_{pzc}$ of SSAB was determined following the solid addition method [36]. Initially, pH of 0.01 M $KNO_3$ solution was adjusted within a pH range of 2–6 followed by addition of 1 g of SSAB. This mixture was agitated properly and final pH of the solution was obtained after 24 h of incubation.

### *Batch sorption studies*

A series of batch adsorption studies of $Fe^{2+}$, $Cu^{2+}$ and $As^{5+}$ from aqueous solution using activated biochar was carried out in 100 mL Erlenmeyer flask containing 30 mL of working solution. Optimization of $Fe^{2+}$, $Cu^{2+}$ and $As^{5+}$ removal was designed with six different process parameters. Effects of pH (2–7), temperature (15–40 °C), adsorbent dose (0.2–1.0 g/L), initial concentration (5–90 mg/L), agitation speed (100–180 rpm) and contact time (15–2160 min) were studied in order to determine optimum parametric condition for maximum removal of these ions from aqueous solutions. All experiments were conducted in triplicate to reduce maximum error occurred during execution of the experiment. Concentrations of $Fe^{2+}$, $Cu^{2+}$ and $As^{5+}$ ions before and after adsorption were calculated using the mass balance equation (Eq. (1)):

$$q = \frac{(C_i - C_F)}{m} V \tag{1}$$

where $q$ is maximum metal uptake at equilibrium (mg/g), $C_i$ and $C_F$ are initial and final metal concentrations in the aqueous solution (mg/L) respectively, $m$ is mass of the adsorbent mixed (g) and $V$ is volume of the metal working solution (L). Percentage of metal ion removal from the aqueous solution after adsorption was calculated using Eq. (2):

$$Removal\ \% = \frac{(C_i - C_F)}{C_i} \times 100 \tag{2}$$

### *Analytical methods*

Concentrations of $Fe^{2+}$, $Cu^{2+}$ and $As^{5+}$ before and after adsorption were measured using a UV–Vis spectrophotometer (REMI UV-2310, Kolkata, India). 1,10-Phenanthroline method [37] was used to determine $Fe^{2+}$ concentration. In this process, hydroxylamine retains iron in its ferrous state. Sodium acetate used maintains pH of the solution within pH 3–9 because phenanthroline binds best within this range with ferrous ions forming reddish orange colour complex. Concentration of ferrous ion was determined at 508 nm.

Polyethyleneimine method [38] was used to determine concentration of $Cu^{2+}$ in the solution because of its ability to form complex with cuprous ions over a wide range of pH. Polyethyleneimine is a colourless solution which when added to copper solution reacts with $Cu^{2+}$ ions and forms a deep blue coloured solution which was detected at 275 nm.

Estimation of $As^{5+}$ was carried out by variamine blue method [39]. In this method, $As^{5+}$ is converted to $As^{3+}$ in presence of potassium iodate forming iodine in the solution which reacts with variamine blue forming a blue coloured solution which was detected at 556 nm.

*Desorption and regeneration study*

Desorption of metal ions from spent adsorbent was studied to examine its re-usability. After adsorption of $Fe^{2+}$, $Cu^{2+}$ and $As^{5+}$ onto SSAB, the spent adsorbent was agitated in a mixture of 1 N HCl, 1 N ethanol, deionized water and tap water for desorption. After metal adsorption, the spent adsorbents were separated from aqueous solution by centrifugation at 5000 rpm and dried at 60 °C for about 30 min inside a hot air oven. About 20 mg of SSAB was mixed in 30 mL of desorbing solutions in 100 mL Erlenmeyer flask and agitated for 360 min at 25 °C. The desorbed samples were separated from aqueous solution by centrifugation and the supernatant obtained was used to determine desorbed metal ion concentration as desorption percentage ($D_p$) using Eq. (3) [40]:

$$D_p\ \% = \left(\frac{m_d}{m_a}\right) \times 100 \tag{3}$$

where $m_d$ is the amount of desorbed metal in mg and $m_a$ is the amount of adsorbed metal in mg.

Regeneration of the desorbed adsorbent was performed to determine its re-adsorption capability. After desorption, the adsorbent was washed thoroughly with deionized water to remove excess of $H^+$ and $OH^-$ ions from the sorbent. The adsorbent was washed with 1 N NaOH for regeneration of SSAB. Adsorption-desorption cycle was repeated for multiple times to analyse the maximum removal efficiency of the spent adsorbent.

## Results and discussion

*Characterization of the adsorbent*

Table 2 represents the proximate analysis of raw biomass and activated biochar of SSAB. It can be seen that activation of the raw biomass has affected its physical characteristics by improvising its efficiency as adsorbent since activation helps in increasing the number of pores on adsorbent surface by subtracting maximum amount of functional groups which might have covered the adsorbent surface. Moisture content, ash content and volatile matter content decreased due to activation, thus, increasing total number of pores on the adsorbent surface. On the other hand, carbon content of SSAB also increased. Characterization of the activated biochar was investigated by physical and instrumental methods. Physical characterization of the adsorbent was analysed in terms of micro-pore volume, total pore volume and surface area by physisorption of $N_2$ on to SSAB at normal boiling temperature (−196.75 °C) in Quanta Chrome Autosorb Automated Gas Adsorption System (ASORP 2PC 1.05). Nitrogen porosimetry principle was used to determine the volume adsorbed to desorbed ratio on SSAB at different $p/p_0$ to obtain its adsorption to desorption ratio value. Dubinin-Radushkevich (DR) equation was applied in deduction of micro pore volume of the activated biochar [41]. Surface micro-morphology of the adsorbent was studied in BET surface analyser (SMART Instruments, India) [25]. Surface area of SSAB was found to be 102.4 $m^2/g$ when the adsorbent was treated with 29.78% of $N_2$ and 71.25% of He. The same mixture of $N_2$ and He was used to determine pore volume of the adsorbent. For pore volume determination, proportion of $N_2$ and He in the gaseous mixture was changed to 94.96% and 5.04% respectively. Micro-pore volume and total pore volume of SSAB obtained were 0.3529 $cm^3/g$ and 0.4053 $cm^3/g$ respectively. This steam activated biochar produced from roots of *C. esculenta* was further used as an adsorbent in metal removal from aqueous solution.

**Table 2** Proximate analysis of raw biomass and activated biochar.

| Properties | Results | |
|---|---|---|
| | Raw biomass weight (%) | Activated biochar weight (%) |
| Moisture content | 10.5 | 3.85 |
| Ash content | 6.93 | 3.67 |
| Volatile content | 74 | 20.65 |
| Fixed carbon content | 19.07 | 75.68 |

*SEM analysis of the adsorbent*

Surface morphological analysis of the adsorbent before and after adsorption was performed in a scanning electron microscope (SEM) (JEOL JSM-6030, Kolkata, India). Before analysis, the samples were coated with palladium (8 nm of thickness) at an application rate of 30 mA for 30 s. Coating of sample was done to enhance the conductivity of the sample under SEM. The sample was coated inside an auto fine coater (JEOL JFC 1600, JEOL INDIA PVT. Ltd., Kolkata, India) followed by drying of the sample using infra red (IR) lamp before it was analysed. SEM images as shown in Fig. 1a–d of SSAB both before and after adsorption for each of $Fe^{2+}$, $Cu^{2+}$ and $As^{5+}$ provide a clear image of numerous pores and greyish crystals of metal ion bonds present on the surface of SSAB. After superheated steam activation, the adsorbent surface was modified with irregular clusters of numerous minute honey comb-like structures making wide space for adhesion. The honey comb-like structures formed were void in nature and were filled with metal ions all along the pores present on the adsorbent surface.

*Fourier transform infrared spectrum analysis of the adsorbent*

Fourier Transform Infrared (Smart Omni Transmission IS 10 FT-IR Spectrometer, Thermo Fisher Scientific, India) analysis of SSAB and metal loaded SSAB was conducted to determine the functional groups present on the adsorbent surface which might be responsible for $Fe^{2+}$, $Cu^{2+}$ and $As^{5+}$ adsorption.

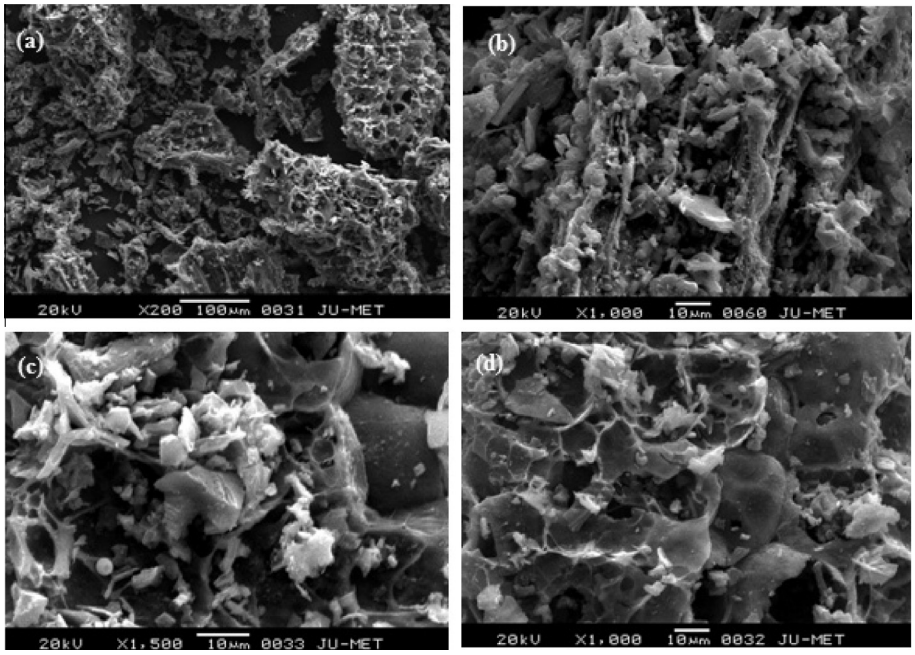


**Fig. 1** SEM image of (a) raw adsorbent and after adsorption of (b) $Fe^{2+}$ (c) $Cu^{2+}$ and (d) $As^{5+}$.

2 mg of each sample was separately mixed with 100 mg of potassium bromide and finely ground. The ground powder was pressed into pellets before the adsorbent was analyzed [40]. The FT-IR spectrum as shown in Fig. 2 exhibits a good number of peaks suggesting various functional groups to be present on the adsorbent surface. When the infrared light interacts with the molecules present on the sample, the functional groups present on it will stretch, bend and contract. Thus, specific functional group will absorb infrared radiation at particular wavelength irrespective of the molecular structure of the sample [42]. Therefore on the basis of this principle, specific functional groups present on SSAB responsible for $Fe^{2+}$, $Cu^{2+}$ and $As^{5+}$ adsorption were studied within the range of 4000–400 $cm^{-1}$. Functional groups such as carboxylic acids, aldehydes and aromatic groups were located within 3400–2400 and 1725–1700 $cm^{-1}$, 2830–2695 $cm^{-1}$ and 3100–3000 $cm^{-1}$ frequencies respectively. Terminal alkynes were found within 3330–3200 $cm^{-1}$ frequency and alcohols and phenols ranging within the stretch of 3500–3640 $cm^{-1}$ were found on the surface of raw SSAB.

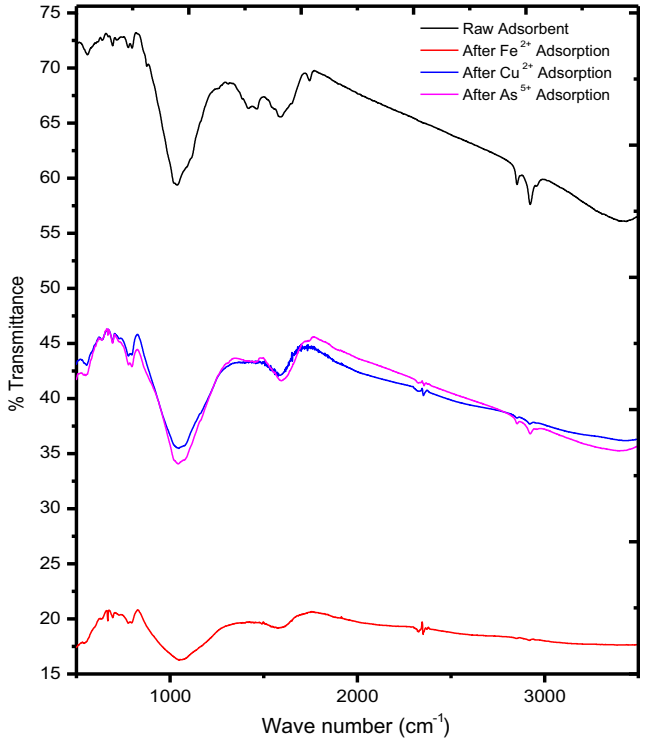


**Fig. 2** FT-IR spectra of SSAB before and after adsorption of $Fe^{2+}$, $Cu^{2+}$ and $As^{5+}$.

FTIR spectrum obtained from spent SSAB illustrates shifting of peaks for all three metal ions suggesting bond formation between the metal ions and adsorbent molecules. In case of spent adsorbent, there was a shifting of the peaks at 3310 $cm^{-1}$ (for $Fe^{2+}$), 3432 $cm^{-1}$ (for $Cu^{2+}$) and 3331 $cm^{-1}$ (for $As^{5+}$). These shifts are quite typical for complexation of metal ions by coordination with phenolic groups [43]. The metal ions formed a bond with medium metal strength forming a metal-oxide (Me-O) by replacing the $H^+$ ion from the phenol group. Apart from the phenolic group, complexation with the carboxylic group was also found. Another shifting occurred at 1677 $cm^{-1}$, 2463 $cm^{-1}$ and 2516 $cm^{-1}$ for $Fe^{2+}$, $Cu^{2+}$ and $As^{5+}$ respectively suggesting involvement of carboxylic acid in metal adsorption. During adsorption of metal on to adsorbent comprising carboxylic functional group on its surface, it undergoes chelation either at *o*-hydroxycarboxylic or at *o*-dicarboxylic sites. It has already been reported that the carboxylic groups present on the adsorbent are responsible for most of the adsorption of metal ions [44]. Thus FTIR analysis of raw SSAB and spent SSAB suggests adsorption of metal ions on to the adsorbent which was facilitated by the carboxylic and phenolic groups present on it.

*Proposed mechanism of $Fe^{2+}$, $Cu^{2+}$ and $As^{5+}$ adsorption on SSAB*

It is important to understand the inherent mechanism of metal adsorption onto adsorbent. Solubility of the solute (adsorbate) and affinity of particular solute ion onto adsorbent are two important resultant driving forces of an adsorption mechanism. These driving forces may be due to the type of bonding which exists between an adsorbent and adsorbate. On this aspect, FTIR analysis helps in understanding the underlying mechanism of an adsorption process. Apart from the functional groups present on SSAB, the above mentioned process parameters also played an important role in culminating the sorptive mechanism. Taking into account, this work presents a description of $Fe^{2+}$, $Cu^{2+}$ and $As^{5+}$ adsorption on to SSAB. The FTIR analysis suggests the presence of carboxylic acids, aldehydes, aromatic groups, terminal alkynes, alcohols and phenols as functional groups on SSAB. Among these functional groups, carboxylic acid and phenol were found to be responsible for adsorption of these metal ions. Carboxylic acid is polar in nature, which donates and accepts both $H^+$ and $OH^-$ groups due to the presence of carbonyl and hydroxyl groups, whereas, phenol consists of both phenyl ($-C_6H_5$) and hydroxyl group (—OH). Presence of multiple functional groups on an adsorbent generates higher possibilities of adsorbate and adsorbent interactions. Metal binds on to adsorbent by complexation and hydrolysis mediated adsorption. Shifting of —OH stretch after metal adsorption suggests hydrogen bonding. In metal adsorption, permanence of complexes is established mostly by the basicity of donor cluster, i.e., greater the basicity, greater is the stability of the complexes. In case of $Cu^{2+}$, $Fe^{2+}$ and $As^{5+}$, the —OH group played an important role in bonding with the adsorbent. In general, metal fixes on to carbon by ligand formation and via ion-exchange. In our study, all the three ions formed ligands with the functional groups by replacing $H^+$ with metal ions creating an organometallic complex on the adsorbent surface as it can be seen in Scheme 1. Though both phenol and carboxylic acid took part in the metal adhesion, the metal ion chemistry and its affinity created an overall difference it their overall uptake [45].

*Optimization of single metal adsorption*

*Point of zero charge $pH_{pzc}$ and effect of pH*

It is important to analyse the point of zero charge of an adsorbent since it determines the pH at which adsorbent surface determines net neutrality of total electric charges. The $pH_{pzc}$ of the activated biochar was found to be 6.2. It was observed that at this particular pH of 6.2, functional groups present on SSAB which might be either acidic or basic in nature will no longer affect pH of the aqueous solution. Therefore, pH of the aqueous solution will influence both adsorbent surface charge and ionization of contaminants. Both $H^+$ and $OH^-$ ions adhere firmly onto the adsorbent's surface, thus affecting the sorption of contaminant ions.

Effect of pH on adsorptive removal of $Fe^{2+}$, $Cu^{2+}$ and $As^{5+}$ using SSAB was studied within the pH range of 2–7. It is shown in Fig. 3a that adsorptive uptake of $Fe^{2+}$, $Cu^{2+}$ and $As^{5+}$ depends highly on pH where with increase or decrease in pH, overall uptake capacity of the adsorbent changed. At lower pH, maximum adsorption of $Fe^{2+}$ was observed. When initial pH of ferrous aqueous solution was increased from pH 2 to 3, a gradual increase in the metal uptake by SSAB was observed. At pH 3, after a steep increment of metal adsorption from pH 2, uptake capacity of SSAB reached its equilibrium with maximum removal of 78.94%. There was a decrease in $Fe^{2+}$ ion adsorption onto SSAB as the pH was increased from 3 to 7. This can be attributed to the fact that the predominant ferrous species $[Fe(H_2O)_6]^{2+}$ found at lower pH fails to interact with adsorbent surface since with increase in pH, the number of $[Fe(OH)(H_2O)_5]^+$ also increases [46,47] thereby leaving lesser surface for ferrous ion to interact with the adsorbent. Due to the increase in $[Fe(OH)(H_2O)_5]^+$ species, precipitation of $Fe^{2+}$ into $Fe(OH)_3$

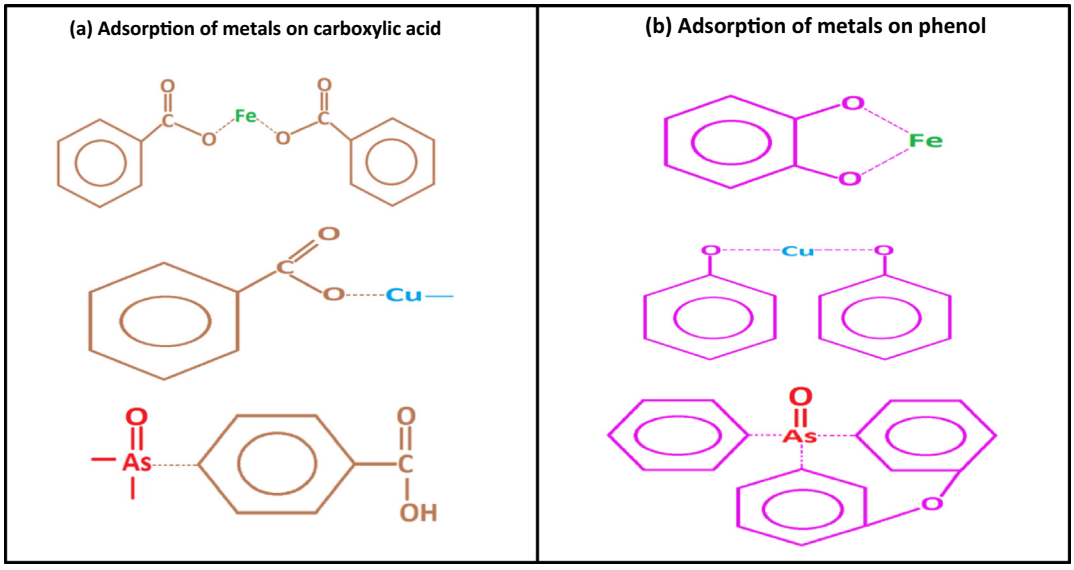


**Scheme 1** Adsorption mechanism of $Fe^{2+}$, $Cu^{2+}$ and $As^{5+}$ on to SSAB. (a) Proposed bonding of $Fe^{2+}$, $Cu^{2+}$ and $As^{5+}$ with carboxylic acid. (b) Proposed bonding of $Fe^{2+}$, $Cu^{2+}$ and $As^{5+}$ with phenol.

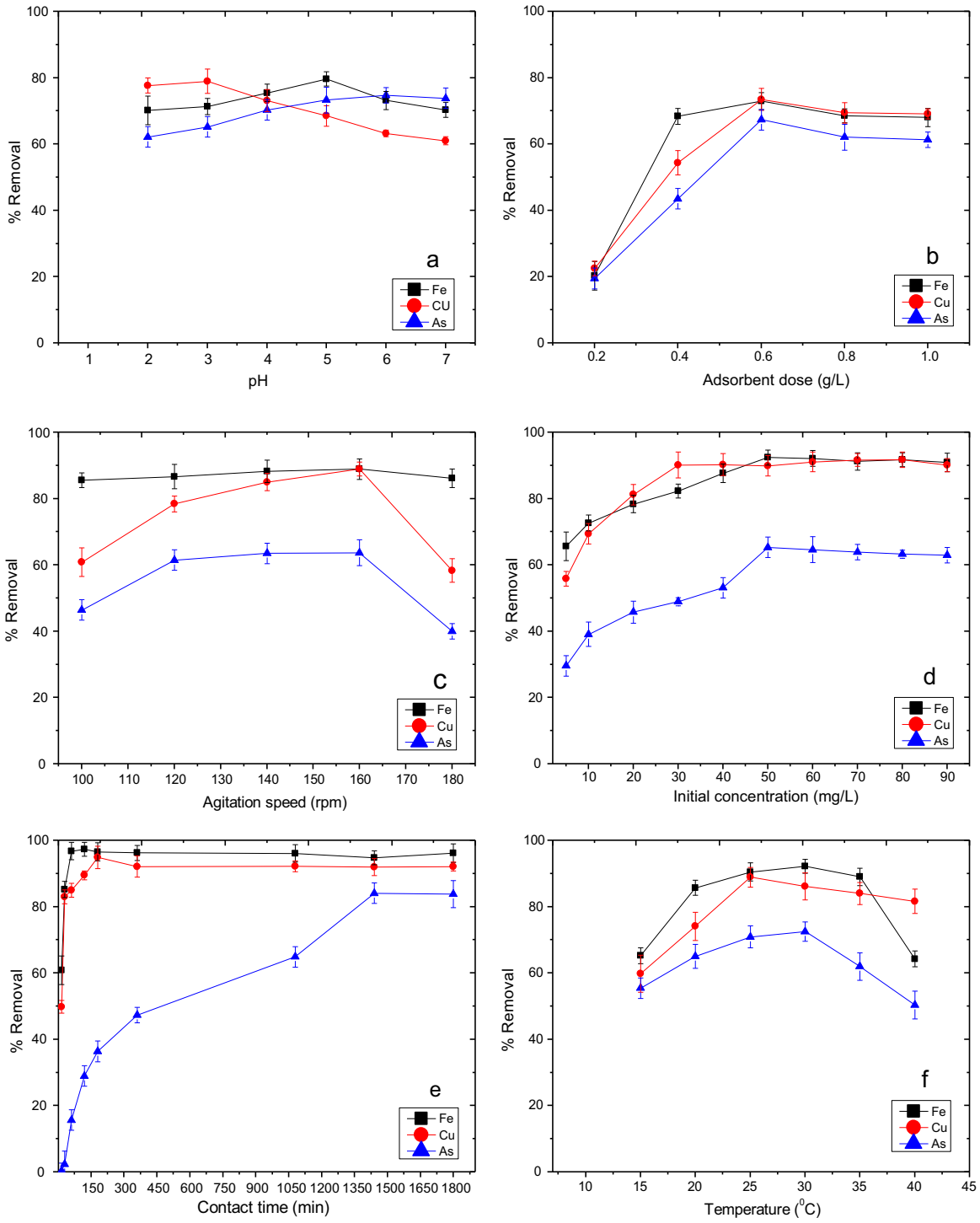


**Fig. 3** Effect of (a) pH, (b) adsorbent dose, (c) agitation speed, (d) initial concentration, (e) contact time, and (f) temperature on $Fe^{2+}$, $Cu^{2+}$ and $As^{5+}$ adsorption.

increases resulting in less adsorption of $Fe^{2+}$ at higher pH [48]. Similarly, adsorption of $Cu^{2+}$ and $As^{5+}$ onto SSAB under the influence of pH was studied. In case of $Cu^{2+}$ and $As^{5+}$, removal percentage increased with increase in pH. In Fig. 3a, it can be clearly seen that at pH 5 and 6, the adsorbent was able to remove $Cu^{2+}$ and $As^{5+}$ with a maximum removal of 79.66% and 74.74% respectively, whereas at lower pH, it was unable to remove $Cu^{2+}$ and $As^{5+}$ at a considerate amount. This may be due to the affinity of SSAB towards $H^+$ ions which increases at higher concentration of $H^+$ ions. This increase in $H^+$ ions prevents bond formation between the heavy metal ions and the adsorbent surface. Thus, it can be clearly said that SSAB has the capability to adsorb various metal contaminants at various pH levels.

*Effect of adsorbent dose*

Adsorbent dose is one of the important factors which affect the adsorption process significantly. In order to determine the effect of adsorbent dose on removal percentage of $Fe^{2+}$, $Cu^{2+}$ and $As^{5+}$, amount of SSAB dose was varied within a range of 0.2–1.0 g/L keeping the adsorbate concentration constant at 10 mg/L. Effect of SSAB dose on removal percentage of $Fe^{2+}$, $Cu^{2+}$ and $As^{5+}$ is shown in Fig. 3b. It followed a predicted manner of increase in metal adsorption with increase in adsorbent dose until it reached a saturation point as the dose was increased to an optimum amount. Among various dosages used, 0.6 g/L of SSAB was observed to be the optimum adsorbent dose showing maximum removal. At lower adsorbent dosage values, adsorption is affected by inter-ionic competition among the adsorbate particles which was more due to presence of lesser surface area of SSAB. As a result of resistance at solid liquid interface, mass transfer of $Fe^{2+}$, $Cu^{2+}$ and $As^{5+}$ became feasible at higher adsorbent dose. Also, removal percentage decreased as the adsorbent dose was increased beyond 0.6 g/L. This might have occurred due to aggregation of adsorbent particles and repulsive action among the binding sites which decreased binding capability between adsorbate and adsorbent leading to a reduction in total number of binding sites on SSAB.

*Effect of agitation speed*

Role of agitation speed in removal of $Fe^{2+}$, $Cu^{2+}$ and $As^{5+}$ from aqueous solution was studied. In Fig. 3c, it can be seen that removal of the metal contaminants was greater at higher agitation speed. Removal of $Fe^{2+}$, $Cu^{2+}$ and $As^{5+}$ was optimum at 160 rpm with 0.6 g/L of adsorbent dose, after which it showed a steady decline in both adsorbance and adsorptivity. Adsorption of $Fe^{2+}$ showed a consistency from 100 to 160 rpm with little variation in overall removal percentage from 85.58% to 88.89%, whereas removal percentage of $Cu^{2+}$ increased gradually with increase in agitation speed until it removed 88.88% at 160 rpm. On the other hand, removal percentage of $As^{5+}$ continued to increase from 61.48% to 63.68% when the agitation speed was increased from 120 to 160 rpm but the differences were very negligible. In case of $Cu^{2+}$ and $As^{5+}$ when the agitation speed was set at 180 rpm, removal percentage decreased as compared to $Fe^{2+}$, where the removal percentage remained constant. Adsorption of $Cu^{2+}$ and $As^{5+}$ decreased at higher agitation speed which might be due to the fact that at elevated speed, these metal ions were unable to bind onto the adsorbent surface. The time required for metal ions to bond with SSAB was less due to high speed thus affecting total metal adsorptivity.

*Effect of initial metal concentration and adsorption isotherm*

Inter-relationship of initial $Fe^{2+}$, $Cu^{2+}$ and $As^{5+}$ concentrations and sorptive efficiency of SSAB were studied with an adsorbent dose of 0.6 g/L. As it shown in Fig. 3d that with increase in initial metal concentration from 5 to 90 mg/L, the rate of adsorption increased with an optimum initial concentration of 50, 30 and 50 mg/L of $Fe^{2+}$, $Cu^{2+}$ and $As^{5+}$ respectively. Adsorption of the three metal contaminants increased gradually with increase in initial concentration. When the initial metal ion concentration was within the range of 5–50 mg/L in case of $Fe^{2+}$ and $As^{5+}$ and 5–30 mg/L for $Cu^{2+}$, there was an increment in the adsorption of $Fe^{2+}$, $Cu^{2+}$ and $As^{5+}$ beyond which there was a saturation in overall adsorptivity of metal ions onto SSAB. When the ratio of metal ion concentration to adsorbent dose is less, higher energy sites present on adsorbent surface are used up for adsorption. Unlikely, when the ratio increases, these higher energy sites overcrowd adsorbent surface leaving little space for lower energy sites to execute remaining adsorption, thus decreasing sorption efficiency of the adsorbent. Maximum removal percentage of $Fe^{2+}$, $Cu^{2+}$ and $As^{5+}$ achieved were 92.39%, 90.12% and 65.3% respectively. Thus, it can be concluded that SSAB can effectively remove most of $Fe^{2+}$, $Cu^{2+}$ and $As^{5+}$ from aqueous solution if the initial metal ion concentration remains within 50 mg/L and 30 mg/L and 50 mg/L of $Fe^{2+}$, $Cu^{2+}$ and $As^{5+}$ respectively.

In order to obtain a better knowledge on adsorption efficiency of an adsorbent, isotherm models give a better explanation of the sorptive process. Adsorption isotherms of the three metal contaminants were developed from batch adsorption study with SSAB as adsorbent. Adsorbance of $Fe^{2+}$, $Cu^{2+}$ and $As^{5+}$ onto SSAB was calculated with different initial metal ion concentrations. Thus, the findings were fitted in Langmuir and Freundlich adsorption isotherm models [49] using Eqs. (4) and (5) as follows:

$$\frac{1}{q_e} = \frac{1}{C_e b q_m} + \frac{1}{q_m} \tag{4}$$

where $q_e$ (mg/g) is the amount of the adsorbate absorbed on per unit mass of the adsorbent at the equilibrium, $q_m$ (mg/g) is the adsorption capacity of adsorbent, $b$ (L/mg) is the adsorption constant interpreted as the amount of free energy capacity of the adsorbent and $C_e$ (mg/L) is the concentration of $Fe^{2+}$, $Cu^{2+}$ and $As^{5+}$ in the aqueous solution at equilibrium.

$$\ln q_e = \ln K_F + \frac{1}{n} \ln C_e \tag{5}$$

where $K_F$ is the adsorption proportionality constant and $n$ is the dimensionless exponential adsorption constant related to the intensity of bond formation between the adsorbate and the adsorbent.

An inter-relationship between the metal contaminants and SSAB was established which suggested a variation in adsorptive behaviour of the adsorbent with initial adsorbate concentration. When $Fe^{2+}$, $Cu^{2+}$ and $As^{5+}$ concentrations in the aqueous solution were increased from 5 to 50 mg/L, adsorptive uptake of the adsorbent also increased. Values obtained from isotherm characterization of the present adsorption study have been listed in Table 3. The $R^2$ values obtained for the three metal ions viz., $Fe^{2+}$, $Cu^{2+}$ and $As^{5+}$ were 0.982, 0.988 and 0.994 for Langmuir and 0.946, 0.963 and 0.941 for Freundlich isotherm model. A comparative study on the maximum adsorptive capacity of $Fe^{2+}$, $Cu^{2+}$ and $As^{5+}$ on to other conventional adsorbent has been listed in Table 4 [49–55]. The values of regression co-efficient ($R^2$) obtained from the isotherm models suggested a monolayer metal adsorption. The values of $q_m$ and $b$ obtained from Langmuir isotherm model for $Fe^{2+}$, $Cu^{2+}$ and $As^{5+}$ removal suggest an appreciable metal uptake capacity of SSAB with little free energy involved in it. The values of $q_m$ suggest an appreciable extended affinity of ferrous ions towards SSAB as compared to cuprous and

**Table 3** Related parameters of Langmuir and Freundlich isotherms obtained from the adsorption of and correlation of $Fe^{2+}$, $Cu^{2+}$ & $As^{5+}$ adsorption onto SSAB.

| Metal ions | Langmuir | | | Freundlich | | |
|---|---|---|---|---|---|---|
| | $q_e$ (mg/g) | $b$ (L/mg) | $R^2$ | $K_f$ (mg/g) | $n$ | $R^2$ |
| $Fe^{2+}$ | 6.19 | 0.353 | 0.982 | 1.25 | 1.28 | 0.946 |
| $Cu^{2+}$ | 2.31 | 0.089 | 0.988 | 1.18 | 1.22 | 0.963 |
| $As^{5+}$ | 2.2 | 0.001 | 0.994 | 0.832 | 1.2 | 0.941 |

**Table 4** Comparison of adsorption capacities of various adsorbents for $Fe^{2+}$, $Cu^{2+}$ and $As^{5+}$.

| Adsorbent used | Mode of modification | Adsorption capacity (mg/g) | | | Reference |
|---|---|---|---|---|---|
| | | $Fe^{2+}$ | $Cu^{2+}$ | $As^{5+}$ | |
| Waste crab shell | Pretreatment with HCl | – | – | 8.3 | [49] |
| Untreated mangos teen shell | – | – | 3.15 | – | [50] |
| Pomegranate peel | Chemically activated by phosphoric acid | – | 5.8 | – | [41] |
| Jute fibres | Chemically oxidized using $H_2O_2$ and NaOH | – | 4.23 | – | [51] |
| Untreated coir fibre | – | 2.03 | – | – | [52] |
| Oxidized coir fibre | Activation using $H_2O_2$ and NaOH | 7.49 | – | – | [52] |
| Activated olive stone | Activation using $K_2CO_3$ and $HNO_3$ and steam | – | – | 0.111 | [53] |
| Activated olive pulp | Activation using $K_2CO_3$ and $HNO_3$ and steam | – | – | 0.129 | [53] |
| *m*-Phenylenediamine | Chemical oxidative polymerization using $(NH_4)_2S_2O_8$ | – | 12.3 | – | [54] |
| *p*-Sulfonic-*m*-phenylenediamine | Chemical oxidative polymerization using $(NH_4)_2S_2O_8$ | – | 28.4 | – | [54] |
| SSAB | Steam activation of biochar produced from roots of *C. esculenta* | 6.19 | 2.31 | 2.2 | [Present work] |

arsenate ions. Also the values of $K_F$ and $n$ were more for ferrous ion than the remaining two metal ions. Therefore the adsorption model suggests that adsorption of these metal contaminants on to surface of SSAB occurred in properly organized sites. These sites were considered to be potentially equivalent while maintaining uniform distance from each other; hence, no intra-molecular interactions were observed. Thus, steam activation of the biochar has helped in developing uniform sites for metal ion adsorption.

*Effect of adsorption time and adsorption kinetics*

Fig. 3e shows the effect of adsorption time on metal uptake of SSAB from the aqueous solutions of $Fe^{2+}$, $Cu^{2+}$ and $As^{5+}$ studied within a time range of 15–2160 min with 0.6 g/L of SSAB. Metal uptake by the adsorbent increased inconsistently with increase in the adsorption time. This clearly states that adsorption of these metal ions was divided into two segments with respect to time, that is, a former rapid step and a subsequent delayed step. Adsorption of $Fe^{2+}$ was faster within the former rapid step of first 30 min with an initial concentration of 50 mg/L, which increased the adsorptive capacity of the adsorbent almost up to 5.82 mg/g with an overall removal of 85.19%. After a time lapse of another 30 min, adsorption efficiency of SSAB increased to an extent of 6.19 mg/g with maximum removal of 97.34% from the aqueous solution. A similar sequence of time lapse was observed in case of $Cu^{2+}$, where maximum removal of 94.89% with an uptake of 2.31 mg/g was observed when the equilibrium reached at 180 min from an initial concentration of 30 mg/L. Therefore it can be said that the former rapid step for both $Fe^{2+}$ and $Cu^{2+}$ occurred at same time interval of 30 min but the remaining $Cu^{2+}$ ions took two hours to reach its equilibrium. On the other hand, the arsenate ions took comparatively more time in adhering on to SSAB. The arsenate ions followed a comparative delayed phase where SSAB took 1440 min to reach its saturation point at 2.2 mg/g where it was able to remove 84.09% from arsenate aqueous solution. From the adsorption trend followed by SSAB during arsenate adsorption, it can be said that in comparison with the other two metal ions it took relatively more time to reach its maxima creating a former delayed step followed by a subsequent rapid step. The former rapid step observed for ferrous and cuprous ions might be due to physical and surface adsorptive phenomenon owing to the presence of surface reactive groups. This surface sorption of the ions onto adsorbent surface might have covered up the pores thus delaying the adsorption rate. The arsenate ions, on the other hand, were not able to adhere themselves onto the SSAB surface in an appreciable rate which might be due to low bonding energy resulting in higher contact time for adsorption.

Adsorption kinetics is considered to be an important criterion in characterizing the adsorption rate of a sorption reaction. It describes the influence of reaction time governing rate of adsorbent uptake. Pseudo-first order and pseudo-second order adsorption kinetic models were used to determine the adsorption kinetics of $Fe^{2+}$, $Cu^{2+}$ and $As^{5+}$ onto SSAB. Eqs. (6)–(8) were used to generate data from the kinetic models [49]:

$$\ln(q_e - q_t) = \ln q_e - b_{ad}t \tag{6}$$

where $q_e$ is the amount of metal adsorbed at equilibrium (mg/g), and $q_t$ is the amount of metal adsorbed at time $t$ (mg/g). $b_{ad}$ is the adsorption constant calculated from the ln $(q_e - q_t)$ vs $t$ plot.

$$\frac{t}{q_t} = \frac{1}{b_2 q_e^2} + \frac{1}{q_e}t \tag{7}$$

$$h = b_2 q_e^2 \quad (8)$$

where $b_2$ is the adsorption constant for pseudo-second kinetics and $h$ is the initial adsorption rate (mg/g min). Tables 5–7 represent the subsequent parameters, which suggest the kinetics of $Fe^{2+}$, $Cu^{2+}$ and $As^{5+}$ adsorption on to SSAB could be more explainable with pseudo-second order kinetic model due to greater regression coefficient ($R^2$). This could be attributed to the rate determining step which was governed by covalently driven forces either by electron exchanges or by valence forces via sharing of electrons at the junction of solid liquid interface. Results suggest the rate of adsorption to be faster due to huge amount of metal adsorption on to SSAB within a short period of time for both ferrous and cuprous ions which was not the same in case of arsenate.

*Effect of temperature and thermodynamics study*

Effect of temperature on metal adsorptivity of SSAB was investigated. In Fig. 3f it can be seen that the adsorptivity of SSAB altered with increase in temperature up to 40 °C. At a moderate temperature range of 25–30 °C, maximum removal of 92.22%, 88.88% and 72.5% of ferrous, cuprous and arsenate ions respectively was observed. Adsorptivity and adsorption of $Fe^{2+}$, $Cu^{2+}$ and $As^{5+}$ decreased as the temperature was increased with an increment of 5 °C up to 40 °C which suggested adsorption of these metal contaminants was favoured at moderate temperature. Interaction between the functional groups present on SSAB and $Fe^{2+}$, $Cu^{2+}$ and $As^{5+}$ was able to form strong bond at this temperature range which reduced with increase in temperature [56]. Thus, the adsorption is exothermic since adsorption and adsorptivity decreased with increase in temperature.

The influence of temperature on adsorptive removal was further investigated in terms of thermodynamic properties viz., Gibbs' free energy (ΔG°), enthalpy (ΔH°) and entropy (ΔS°). These thermodynamic parameters were established from the experimental output obtained from the following Eqs. (9) and (10):

$$\Delta G^\circ = -RT \ln b_a \quad (9)$$

where $R$ is the universal gas constant with the value of $8.314 \times 10^{-3}$ kJ/mol K, $T$ is the absolute temperature in Kelvin (K), $b_a$ is the adsorption constant at equilibrium derived from Langmuir isotherm model at corresponding temperature, $\Delta H^\circ$ (kJ/mol), $\Delta S^\circ$ (kJ/mol K) and $\Delta G^\circ$ (kJ/mol) are the enthalpy, entropy and Gibbs free energy respectively. Gibbs free energy at respective temperature was calculated from Eq. (9) and the change in enthalpy and entropy was calculated from Eq. (10):

$$\Delta H^\circ = \Delta G^\circ + T\Delta S^\circ \quad (10)$$

From the slope and intercept of $\Delta G^\circ$ and $T$ plot as shown in Fig. 4, the values of $\Delta H^\circ$ and $\Delta S^\circ$ were obtained. Values of $\Delta H^\circ$ and $\Delta S^\circ$ were found to be negative. Negative values of $\Delta H^\circ$ suggested the adsorption process to be exothermic in nature. On the other hand, negative values of $\Delta S^\circ$ suggested decrease in affinity of the metal ions with increase in

**Table 5** Calculated parameters of pseudo-first order and pseudo-second order for $Fe^{2+}$ adsorption.

| Metal ion | Initial conc. (mg/L) | Pseudo-first order | | | | Pseudo-second order | | | |
|---|---|---|---|---|---|---|---|---|---|
| | | $q_e$ (exp) (mg/g) | $q_e$ (cal) (mg/g) | $b_{ad}$ | $R^2$ | $q_e$ (cal) (mg/g) | $b_2$ | $h$ (mg/g min) | $R^2$ |
| $Fe^{2+}$ | 5 | 2.245 | 1.181 | 0.005 | 0.993 | 2.02 | 0.122 | 0.853 | 0.998 |
| | 10 | 2.46 | 1.691 | 0.018 | 0.974 | 2.15 | 0.362 | 1.32 | 0.999 |
| | 30 | 3.9 | 3.167 | 0.022 | 0.99 | 3.42 | 0.664 | 2.76 | 0.999 |
| | 50 | 6.195 | 5.110 | 0.018 | 0.991 | 6.62 | 0.671 | 3.3 | 0.993 |

**Table 6** Calculated parameters of pseudo-first order and pseudo-second order for $Cu^{2+}$ adsorption.

| Metal ion | Initial conc. (mg/L) | Pseudo-first order | | | | Pseudo-second order | | | |
|---|---|---|---|---|---|---|---|---|---|
| | | $q_e$ (exp) (mg/g) | $q_e$ (cal) (mg/g) | $b_{ad}$ | $R^2$ | $q_e$ (cal) (mg/g) | $b_2$ | $h$ (mg/g min) | $R^2$ |
| $Cu^{2+}$ | 5 | 2.56 | 0.1 | 0.005 | 0.992 | 2.49 | 0.039 | 5.43 | 0.991 |
| | 10 | 2.41 | 0.418 | 0.008 | 0.988 | 2.22 | 0.033 | 4.91 | 0.999 |
| | 30 | 2.31 | 1.02 | 0.01 | 0.993 | 2.02 | 0.023 | 3.80 | 0.998 |
| | 50 | 2.31 | 1.188 | 0.011 | 0.991 | 1.99 | 0.01 | 3.45 | 0.996 |

**Table 7** Calculated parameters of pseudo-first order and pseudo-second order for $As^{5+}$ adsorption.

| Metal ion | Initial conc. (mg/L) | Pseudo-first order | | | | Pseudo-second order | | | |
|---|---|---|---|---|---|---|---|---|---|
| | | $q_e$ (exp) (mg/g) | $q_e$ (cal) (mg/g) | $b_{ad}$ | $R^2$ | $q_e$ (cal) (mg/g) | $b_2$ | $h$ (mg/g min) | $R^2$ |
| $As^{5+}$ | 5 | 3.705 | 2.18 | 0.001 | 0.989 | 3.024 | 0.671 | 10.41 | 0.991 |
| | 10 | 3.46 | 1.24 | 0.018 | 0.974 | 2.22 | 0.287 | 3.3 | 0.999 |
| | 30 | 2.9 | 1.16 | 0.022 | 0.990 | 2.77 | 0.017 | 0.09 | 0.999 |
| | 50 | 2.20 | 0.18 | 0.005 | 0.980 | 2.2 | 0.021 | 0.004 | 0.999 |

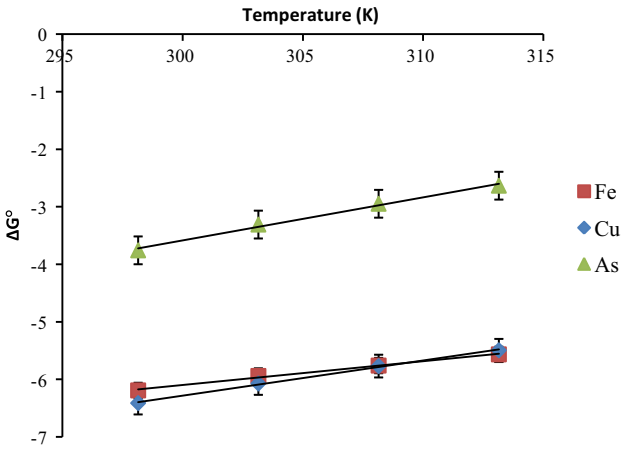


**Fig. 4** Graphical representation of thermodynamic study of $Fe^{2+}$, $Cu^{2+}$ and $As^{5+}$ at pH: 3, 5 and 6; contact time: 60, 180 and 1440 min; temp.: 20–40 °C; initial conc.: 50, 30 and 50 mg/L; adsorbent dose: 0.6 g/L respectively.

temperature. Randomness of metal solution and the adsorbent at solid-liquid interface decreases during adsorption. Negative values of $\Delta G°$ indicated the process to be spontaneous and feasible in nature, where the value of $\Delta G°$ increases with increase in temperature as seen in Table 8, suggesting less availability of metal species. Therefore, with rise in temperature, impact of adsorption phenomenon decreases due to decrease in affinity and spontaneity of the process.

It is essential to determine the method of adsorption mechanism viz., chemisorptions or physisorption, in an adsorption study. Physisorption or physical adsorption refers to a comparative weaker interface where the adsorbate adheres on to the adsorbent surface via van deer Waals force, whereas chemisorption or chemical adsorption is regarded to be firmer due to exchange of electrons within the adsorbate and adsorbent forming chemical bonds. This bond formation causes increase or decrease in surrounding temperature leading to the change in enthalpy ($\Delta H°$) of the system. Therefore change in enthalpy can be considered to be the mode determining factor of an adsorption mechanism. An adsorption process is considered to be exothermic ($-\Delta H°$) when most of the energy gets released into the surrounding due to lack of bond formation between the adsorbate and adsorbent suggesting the process to obey physisorption. On the other hand, in endothermic reaction, the system temperature falls from surrounding temperature due to consumption of more energy in forming chemical bonds between adsorbate and adsorbent suggesting the process to follow chemisorptions. Consequently the present thermodynamic study on the adsorption of $Fe^{2+}$, $Cu^{2+}$ and $As^{5+}$ on to SSAB suggests a physisorption process with maximum adsorption within 25–30 °C. Also it can be said that inefficiency of the adsorption process at higher temperature was due to the alteration of system enthalpy, suggesting accumulation of heat in the surrounding; thus reducing the chances of bond formation and its stability [57].

### *Desorption and regeneration study*

A study on desorption of SSAB is shown in Fig. 5a. It can be seen that the rate of desorption was high for each metal adsorbate when spent SSAB was treated with 1 N HCl. SSAB was then used for multiple cycles of desorption and re-adsorption study with an intermediate step of regeneration. As illustrated in Fig. 5b, the efficacy of SSAB retained after each desorption cycle when it was treated with 1 N NaOH, but it decreased each time when the adsorbent was reused for adsorption without regeneration as seen in Fig. 5c. Hence the removal percentage decreased from 97.24%, 94.89% and 87.94% to 60.8%, 66.34% and 71.2 % for $Fe^{2+}$, $Cu^{2+}$ and $As^{5+}$ respectively when the desorbed adsorbent was used without regenerating it. In desorption, most of $Fe^{2+}$, $Cu^{2+}$ and $As^{5+}$ got substituted with $H^+$ ions of acid which were obtained from the supernatant of desorption solution. Again, pH of metal solution decreased during re-adsorption study owing to the presence of excess $H^+$ ions on SSAB which got replaced by $Fe^{2+}$, $Cu^{2+}$ and $As^{5+}$ ions. Therefore, this excess discharge of $H^+$ ions resulted in decrease in overall solution pH, which eventually lowered the removal percentage of $Fe^{2+}$, $Cu^{2+}$ and $As^{5+}$. Thus SSAB showed possibilities of re-adsorption without major loss in its adsorption efficiency.

### *Cost estimation of SSAB production*

Successful implementation of technique for sorptive removal of contaminants from aqueous solution in commercial field depends largely on the cost of adsorbent production. This study of adsorptive removal of $Fe^{2+}$, $Cu^{2+}$ and $As^{5+}$ concentrates on the use of an activated biocharred adsorbent indigenously derived from unwanted weed *C. esculenta*. No maintenance cost of precursor and curbing the problem of deforestation due to robust growth of this weed are the two most important factors governing adsorbent selection. Therefore, the cost of adsorbent preparation from *C. esculenta* is of great importance. The cost involved in production of activated biochar from *C. esculenta* has not been reported yet as per literature review. Production cost of adsorbent consists of various steps viz., collection, preparation of adsorbent and reusability. Overall expenditure on the adsorbent preparation thus affects its usage at commercial level. Cost estimation of preparing 1 kg SSAB is calculated in Indian rupee (INR) which is as follows:

**Table 8** Related parameters of thermodynamic study obtained from the adsorption of $Fe^{2+}$, $Cu^{2+}$ and $As^{5+}$ onto SSAB.

| Metal ions | $\Delta G°$ (kJ/mol) | | | | $\Delta H°$ (kJ/mol) | $\Delta S°$ (kJ/mol K) | $R^2$ |
|---|---|---|---|---|---|---|---|
| | 25 °C | 30 °C | 35 °C | 40 °C | | | |
| $Fe^{2+}$ | −6.192 | −5.940 | −5.759 | −5.565 | −18.46 | −0.041 | 0.994 |
| $Cu^{2+}$ | −6.411 | −6.071 | −5.768 | −5.494 | −24.61 | −0.061 | 0.997 |
| $As^{5+}$ | −3.757 | −3.309 | −2.947 | −2.633 | −25.98 | −0.074 | 0.993 |

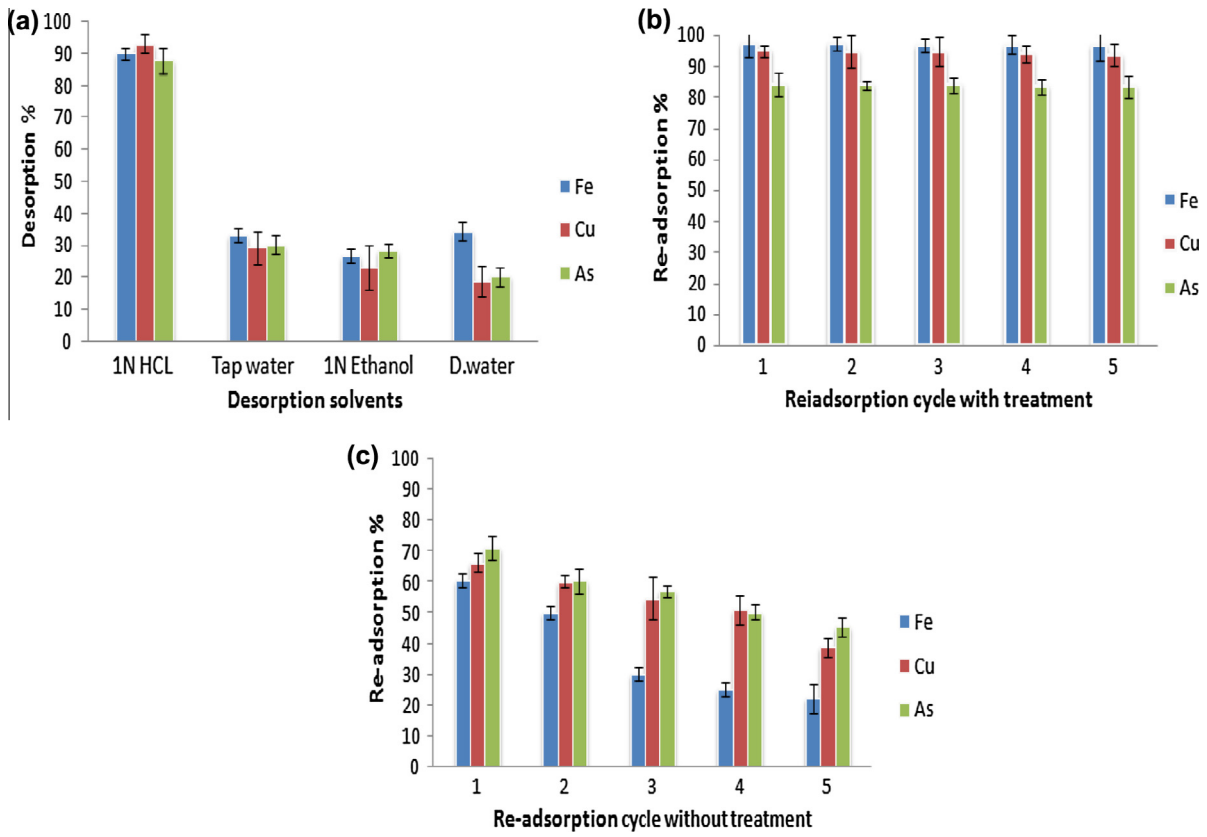


**Fig. 5** (a) Desorption study of the adsorbent after adsorption. (b) Regeneration–adsorption cycle with 1 N NaOH treatment. (c) Regeneration–adsorption cycle without 1 N NaOH treatment (each experiment was conducted with adsorbent dose: 0.6 g/L of SSAB; contact time: 360 min; temp.: 25 °C).

I. Cost of raw material (CRM) = 0.0 INR, since the raw material is locally and abundantly available near water bodies.
II. Cost of size reduction (CSR) = 0.0 INR, since the size reduction was processed manually, but in case of commercial production 10% extra charge should be added to the overall cost.
III. Cost of cleaning raw material (CCRM) = (CH) + (CW) = 2.23 INR, the raw material was washed with distilled water obtained from laboratory setup.
where CH = cost of heating (electricity consumption for 1 L distillation unit × cost of 1 unit) = 0.5 × 4.66 = 2.23 INR.
CW = cost of water usage (tap water was used) = 0.0 INR.
IV. Cost of drying raw material (DRM) = hours × units × per unit cost = 12 × 1 × 4.46 = 53.52 INR.
V. Cost of carbonization (CC) = CH = cost of heating = hours × units × per unit cost = 1.5 × 3 × 4.46 = 20.07 INR.
VI. Cost of superheated steam activation (CSSA) = (CS) + (CH) = 2.23 + 13.38 = 15.61 INR.
where CS = cost of superheated steam generation = hour × units × unit per cost = 1 × 0.5 × 4.46 = 2.23 INR.
CH = cost of heating = hour × units × per unit cost = 1.5 × 2 × 4.46 = 13.38 INR.
VII. Cost of sample grinding (CSG) = 0.0 INR, the steam activated biochar was ground manually using a motor and pestle.

Therefore, the overall cost for SSAB production = CRM + CSR + CCRM + DRM + CC + CSSA + CSG = 91.43 INR.

Overhead charge = 10% of overall cost = 0.1 × 91.43
= 9.143 INR.

Net cost of SSAB production = 91.43 + 9.14 = 100.57 INR.

Cost estimation of SSAB production suggests that adsorbent preparation from the roots of *C. esculenta* is a cost effective process. Net cost for SSAB production was only 100.57 INR, compared to other activated carbon products derived from plant biomass [58]. With 1 kg of SSAB, 1.5 tons of metal contaminated water can be treated. Thus, activated biochar developed from roots of *C. esculenta* can be used as a cost-effective adsorbent for metal removal from aqueous solution.

## Conclusions

In the present study, superheated steam activated biochar from *C. esculenta* was developed to investigate its efficiency in removal of iron ($Fe^{2+}$), copper ($Cu^{2+}$) and arsenic ($As^{5+}$)

from simulated coal mine wastewater under the influence of various parameters such as pH, temperature, adsorbent dosage, initial metal concentration, contact time and agitation speed. The findings of the present investigation are summarized as follows:

- SSAB was capable of removing 97.34% of $Fe^{2+}$, 94.89% of $Cu^{2+}$ and 84.09% of $As^{5+}$ from aqueous solutions.
- Adsorption of these ions onto SSAB followed monolayer adsorption with maximum uptake of 6.19 mg/g, 2.31 mg/g and 2.2 mg/g at initial concentrations of 50 mg/L, 30 mg/L and 50 mg/L for $Fe^{2+}$, $Cu^{2+}$ and $As^{5+}$ respectively.
- The kinetics of metal adsorption onto SSAB obeyed pseudo-second order model.
- Thermodynamic study revealed spontaneity and exothermic nature of the removal process for $Fe^{2+}$, $Cu^{2+}$ and $As^{5+}$.
- In case of $Fe^{2+}$, metal uptake increased with increase in initial concentration whereas the reverse was observed for $Cu^{2+}$ and $As^{5+}$.
- Desorption and regeneration cycle indicated that maximum desorption was possible with hydrochloric acid and sodium hydroxide thereby maintaining the efficacy of the adsorbent up to 5 cycles.
- In contrast to the increased price and higher consumption of electricity, the cost of SSAB production was found to be quite less as compared to earlier reports on adsorbent preparation from plant biomass.

After all adsorption and desorption studies, SSAB can be considered to be an efficient, cost-effective adsorbent for removal of metal contaminants from simulated coal mine wastewater.

## Conflict of Interest

*The authors have declared no conflict of interest.*

## Compliance with Ethics Requirements

*This article does not contain any studies with human or animal subjects.*

## Acknowledgements

Authors would like to convey their sincere thanks to the Department of Biotechnology, Govt. of India, through Project No: BT/484/NE/TBP/2013 for the financial support towards successful execution of the project. Authors are also thankful to the Department of Chemical Engineering, National Institute of Technology, Durgapur, India, for providing the infrastructural and instrumental support to study this significant research.

## References

[1] Ahmad MK, Islam S, Rahman S, Haque MR, Islam MM. Heavy metals in water, sediment and some fishes of Buriganga River, Bangladesh. Int J Environ Res 2010;4:321–32.
[2] Momodu MA, Anyakora CA. Heavy metal contamination of ground water: The Surulere case study. Res J Environ Earth Sci 2010;2:39–43.
[3] Celik A, Demirbas A. Removal of heavy metal ions from aqueous solutions via adsorption onto modified lignin from pulping wastes. Energy Sources 2005;27:1167–77.
[4] Heydari MM, Abasi A, Rohani SM, Hosseini SMA. Correlation study and regression analysis of drinking water quality in Kashan City, Iran. Middle East J Sci Res 2010;13:1238–44.
[5] Egiebor NO, Oni B. Acid rock drainage formation and treatment: a review. Asia-Pac J Chem Eng 2007;2:47–62.
[6] Prasanna MV, Praveena SM, Chidambaram S, Nagarajan R, Elayaraja A. Evaluation of water quality pollution indices for heavy metal contamination monitoring: a case study from Curtin Lake, Miri City, East Malaysia. Environ Earth Sci 2012;67:1987–2001.
[7] UNEP. United Nations Environmental Programme. Industry and Environment Office, Paris; 1989.
[8] Gupta P, Agarwal S, Gupta I. Assessment of physic-chemical parameters of various lakes of Jaipur, Rajasthan, India. Ind J Fundam Appl Life Sci 2011;1:246–8.
[9] Kritzberg ES, Ekstrom SM. Increasing iron concentration in surface water – factor behind brownification? Biogeosciences 2012;9:1465–78.
[10] Zietz BP, deVergara JD, Dunkelberg H. Copper concentrations in tap water and possible effects on infants health-results of a study in Lower Saxony, Germany. Environ Res 2003;92:129–38.
[11] Mohan D, Pittman CU. Arsenic removal from water/wastewater using adsorbents – a critical review. J Hazard Mater 2007;142:1–53.
[12] James D, Cook MD. Determinants of nonheme iron adsorption in man. Food Technol 1983:124–6.
[13] Dikshith TSS. Safe use of chemicals: a practical guide, United States of America. USA: CRC Press; 2009.
[14] Saha KC, Dikshit AK, Bandyopadhyay MA. A review of arsenic poisoning and its effect on human health. Environ Sci Technol 1999;29:281–313.
[15] Veglio F, Beolchini F. Removal of metals by biosorption: a review. Hydrometal 1997;44:301–16.
[16] Dabrowski A, Hubicki Z, Podkoscielny P, Robens E. Selective removal of the heavy metal ions from water and industrial wastewaters by ion-exchange method. Chemosphere 2004;56:91–106.
[17] Juang RS, Shiau RC. Metal removal from aqueous solutions using chitosan-enhanced membrane filtration. J Membr Sci 2000;165:159–67.
[18] Bakalar T, Bugel M, Gajdosova L. Heavy metal removal using reverse osmosis. Acta Montan Slovaca 2009;14:250–3.
[19] Matlock MM, Howerton BS, Atwood DA. Chemical precipitation of heavy metals from acid mine drainage. Water Res 2002;36:4757–64.
[20] Salam OEA, Reiad NA, ElShafei MA. A study of the removal characteristics of heavy metals from wastewater by low-cost adsorbents. J Adv Res 2011;2:297–303.
[21] Davila JS, Matos CM, Cavalcanti MR. Heavy metals removal from wastewater by using activated peat. Water Technol 1992;26:2309–12.
[22] Wilde EW, Benemann JR. Bioremoval of heavy metals by the use of microalgae. Biotechnol Adv 1993;11:781–812.
[23] Volesky B, Holan ZR. Biosorption of heavy metals. Biotechnol Prog 1995;11:235–50.
[24] Saeed A, Iqbal M, Akhtar MW. Application of biowaste materials for the sorption of heavy metals in contaminated aqueous medium. Pakistan J Sci Ind Res 2002;45:206–11.
[25] Halder GN, Sinha K, Dhawane S. Defluoridation of wastewater using powdered activated carbon developed from *Eichornia crassipes* stem: optimization by response surface methodology. Desalin Water Treat 2015;56:953–66.
[26] Ahmed S, Khalid N, Daud M. Adsorption studies of lead minerals from aqueous media. Sep Sci Technol 2002;37:343–62.

[27] Ravindran V, Stevens MR, Badriyha BN, Pirbazari M. Modeling the sorption of toxic metals on chelant impregnated adsorbent. AIChE J 1999;45:1135–46.
[28] Schneider IAH, Rubio J. Sorption of heavy metal ions by the nonliving biomass of freshwater macrophytes. Environ Sci Technol 1999;33:2213–7.
[29] Lesmana SO, Febriana N, Soetaredjo FE, Sunarso J, Ismadji S. Studies on potential applications of biomass for the separation of heavy metals from water and wastewater. Biochem Eng J 2009;44:19–41.
[30] Qaiser S, Saleem AR, Ahmed MM. Heavy metal uptake by agro based waste materials. Environ Biotechnol 2007;10:1–8.
[31] Wankasi D, Horsfall M, Spiff AI. Sorption kinetics of $Pb^{2+}$ and $Cu^{2+}$ ions from aqueous solution by Nipah palm (*Nypa fruticans* Wurmb) shoot biomass. Electron J Biotechnol 2006;9:587–92.
[32] Davar F, Majedi A, Mirzaei A. Green synthesis of ZnO nanoparticles and its application in the degradation of some dyes. J Am Ceram Soc 2015;98:1739–46.
[33] Onayemi O, Nwigwe NC. Effect of processing on the oxalate content of cocoyam. Food Technol 1987;20:293–5.
[34] Parikh J, Channiwala SA, Ghoshal GK. A correlation for calculating elemental composition from proximate analysis of biomass materials. Fuel 2007;86:1710–9.
[35] Ash B, Satpathy D, Mukherjee PS, Nanda B, Gumaste JL, Mishra BK. Characterization and application of activated carbon prepared from waste coir pith. J Sci Ind Res 2006;65:1008–12.
[36] Balistrieri LS, Murray JW. The surface chemistry of goethite (—FeOOH) in major ion seawater. Am J Sci 1981;281:788–806.
[37] Harvey AE, Smart JA, Amis ES. Simultaneous spectrometric determination of iron (II) and total iron with 1, 10-phenanthroline. Anal Chem 1955;27:26–9.
[38] Jin J, Aihua W, Shengji L. Spectrometry recognition of polyethyleneimine towards heavy metal ions. Colloid Surface A 2014;44:1–7.
[39] Narayana B, Cherian T, Mathew M, Pasha C. Spectrophotometric determination of arsenic in environmental and biological samples. Indian J Chem Technol 2006;33:36–40.
[40] Ibrahim MNM, Ngah WSW, Norliyana MS, Daud WRW, Rafatullah M, Sulaiman O, Hashim R. A novel agricultural waste adsorbent for the removal of lead (II) ions from aqueous solutions. J Hazard Mater 2010;182:357–65.
[41] Nadeem R, Ansari TM, Khalid Am. Fourier transform infrared spectroscopic characterization and optimization of Pb (II) biosorption by fish (*Labeo rohita*) scales. J Hazard Mater 2008:64–73.
[42] Saiz-Jimenez C, Shafizadeh F. Iron and copper binding fungal phenolic polymers: an electron spin resonance study. Curr Microbiol 1984;10:281–6.
[43] Khokhar S, Apenten RKO. Iron binding characteristics of phenolic compounds: some tentative structures – a activity relations. Food Chem 2003;81:133–40.
[44] Repo E, Warchol JK, Bhatnagar A, Silanpaa M. Heavy metals adsorption by novel EDTA-modified chitosan–silica hybrid materials. J Colloid Interf Sci 2011;358:261–7.
[45] Al-Ghouti MA, Li J, Salam Y, Al-Laqtah N, Walker G, Ahmad MNM. Adsorption mechanism of removing heavy metals and dyes from aqueous solution using date pits solid adsorbent. J Hazard Mater 2010;176:510–20.
[46] Dinesh M, Charles JUP. Activated carbons and low cost adsorbents for remediation of tri- and hexavalent chromium from water, review. J Hazard Mater 2006;137:762–811.
[47] Hove M, Hille RVP, Alison EL. Iron solids formed from oxidation precipitation of ferrous sulphate solutions. AIChE J 2007;53:2569–77.
[48] Panday KK, Prasad G, Singh VN. Copper (II) removal from aqueous solutions by fly ash. Water Res 1985;19:869–73.
[49] Niu CH, Volesky B, Cleiman D. Biosorption of arsenic (V) with acid washed crab shells. Water Res 2007;41:2473–8.
[50] Zein R, Suhaili R, Eamestly F, Munaf E. Removal of Pb (II), Cd (II) and Co(II) from aqueous solution using *Garcinia mangstana L.* fruit shell. J Hazard Mater 2010;181:52–6.
[51] EL-Ashtoukhy ESZ, Amin N, Abdelwahab O. Removal of lead (II) and copper (II) from aqueous solution using pomegranate peel as a new adsorbent. Desal 2008;223:162–73.
[52] Shukla S, Pai RS. Adsorption of Cu (II), Ni (II) and Zn (II) on modified jute fibres. Bioresour Technol 2005;96:1430–8.
[53] Shukla S, Pai RS, Shendarkar AD. Adsorption of Cu (II), Ni (II) and Zn (II) and Fe (II) on modified coir fibres. Sep Purif Technol 2006;47:141–7.
[54] Budinova T, Petrov, Razvigorova M, Parra J, Galiatsatou P. Removal of arsenic (III) from aqueous solution by activated carbons prepared from solvent extracted olive pulp and olive stones. Ind Eng Chem Res 2006;45:1896–901.
[55] Huang MR, Lu HJ, Li XG. Synthesis and strong heavy-metal ion sorption of copolymer microparticles from phenylenediamine and its sulfonate. J Mater Chem 2012;22:17685–99.
[56] Li XG, Liao Y, Huang MR, Kaner RB. Interfacial chemical oxidative synthesis of multifunctional polyfluoranthene. Chem Sci 2015;6:2087–101.
[57] Chowdhury S, Saha P. Adsorption thermodynamics and kinetics of malachite green onto $Ca(OH)_2$ treated fly ash. J Environ Eng 2011;137:388–97.
[58] Maheshwari U, Gupta S. Kinetic and equilibrium studies of Cr (VI) removal from aqueous solutions using activated neem bark. Res J Chem Environ 2011;15:939–43.